Journal of Asian Earth Sciences 73 (2013) 284–295

Contents lists available at SciVerse ScienceDirect

Journal of Asian Earth Sciences

journal homepage: www.elsevier.com/locate/jseaes

Ages of sediment-hosted Himalayan Pb–Zn–Cu–Ag polymetallic deposits in the Lanping basin, China: Re–Os geochronology of molybdenite and Sm–Nd dating of calcite

Jinrang Zhang [a,b], Hanjie Wen [a,*], Yuzhuo Qiu [a,c], Yuxu Zhang [a], Chao Li [d]

[a] State Key Laboratory of Ore Deposit Geochemistry, Institute of Geochemistry, Chinese Academy of Sciences, Guiyang 550002, China
[b] Graduate University of Chinese Academy of Sciences, Beijing 100039, China
[c] Key Laboratory for Mineralogy and Metallogeny, Guangzhou Institute of Geochemistry, Chinese Academy of Science, Guangzhou 510640, China
[d] State Center of Geological Experiment and Analysis, Beijing 100037, China

ARTICLE INFO

Article history:
Received 15 August 2012
Received in revised form 16 April 2013
Accepted 29 April 2013
Available online 16 May 2013

Keywords:
Mineralization epoch
Calcite Sm–Nd age
Molybdenite Re–Os dating
Sediment-hosted Pb–Zn–Cu–Ag deposits
Lanping basin
China

ABSTRACT

The Lanping basin is a significant Pb–Zn–Cu–Ag mineralization belt of the Sanjiang Tethyan metallogenic province in China. Over 100 thrust-controlled, sediment-hosted, Himalayan base metal deposits have been discovered in this basin, including the largest sandstone-hosted Pb–Zn deposit in the world (Jinding), and several Cu ± Ag ± Co deposits (Baiyangping, Baiyangchang and Jinman). These deposits, with total reserves of over 16.0 Mt Pb + Zn, 0.6 Mt Cu, and 7000 t Ag, are mainly hosted in Meso-Cenozoic mottled clastic rocks, and strictly controlled by two Cenozoic thrust systems developed in the western and eastern segments of the Lanping basin.

To define the metallogenic history of the study area, we dated nine calcite samples associated with copper sulfides from the Jinman Cu deposit by the Sm–Nd method and five molybdenite samples from the Liancheng Cu–Mo deposit by the Re–Os method. The calcite Sm–Nd age for the Jinman deposit (58 ± 5 Ma) and the molybdenite Re–Os age for the Liancheng deposit (48 ± 2 Ma), together with previously published chronological data, demonstrate (1) the Cu–Ag mineralization in the western Lanping basin mainly occurred in three episodes (i.e., ~56–54, 51–48, and 31–29 Ma), corresponding to the main- and late-collisional stages of the Indo–Asian orogeny; and (2) the Pb–Zn–Ag (±Cu) mineralization in the eastern Lanping basin lacked precise and direct dating, however, the apatite fission track ages of several representative deposits (21 ± 4 Ma to 32 ± 5 Ma) may offer some constraints on the mineralization age.

1. Introduction

The Lanping basin (Fig. 1a) is located at the junction of the Eurasian and Indian Plates, in the eastern Tibetan Plateau, between the Lancangjiang suture and the Jinshajiang–Ailaoshan suture. The Lanping basin is a significant and representative Pb–Zn–Cu–Ag mineralization belt of the Sanjiang Tethyan metallogenic province in China, which possessed much economic potential and produced numerous economically significant deposits.

A series of Cenozoic base metal deposits occur in this basin, including the largest sandstone-hosted Pb–Zn deposit in the world (Jinding, with a reserve of 200 Mt ore, grading 6.08% Zn and 1.29% Pb) and several Cu ± Ag ± Co deposits (Baiyangping, Baiyangchang, and Jinman), located in the northern segment of the basin (Fig. 1b; Hou et al., 2006, 2008; Xue et al., 2007; Khin et al., 2007; He et al., 2009). These deposits, yielding total reserves of over 16.0 Mt Pb + Zn, 0.6 Mt Cu, and 7000 t Ag, are hosted by Meso-Cenozoic mottled clastic rocks, and strictly controlled by the Cenozoic thrust systems related to the Indo-Asian collision since the Paleocene (He et al., 2004; Xu and Zhou, 2004). Spatially, these base metal deposits are divided into two sub-parallel metallogenic belts, which are characterized by sediment-hosted Cu–Ag polymetallic deposits in the western Lanping basin, and Pb–Zn polymetallic deposits in the eastern Lanping basin (Xue et al., 2007; Hou et al., 2008; He et al., 2009).

These sediment-hosted, Himalayan base deposits in the Lanping basin are controlled by thrust–nappe structures and formed in the Himalayan continent–continent collisional orogen, which distinguish them from other sediment-hosted base metal deposits in the world (Misra, 2000; Hou et al., 2006; Xue et al., 2007).

The genesis of these sediment-hosted Pb–Zn–Cu–Ag deposits, especially the large to supergiant Jinding and Baiyangping Pb–Zn–Ag (±Cu) deposits, has been extensively studied in the last three decades (e.g. Shi et al., 1983; Qin and Zhu, 1991; Luo and Yang, 1994; Kyle and Li, 2002; Xue et al., 2003, 2007). However, as yet no agreement has been reached on their genesis. One of the most important reasons is the paucity of reliable age data

* Corresponding author.
E-mail address: wenhanjie@vip.gyig.ac.cn (H. Wen).

1367-9120/$ - see front matter © 2013 Elsevier Ltd. All rights reserved.
http://dx.doi.org/10.1016/j.jseaes.2013.04.041

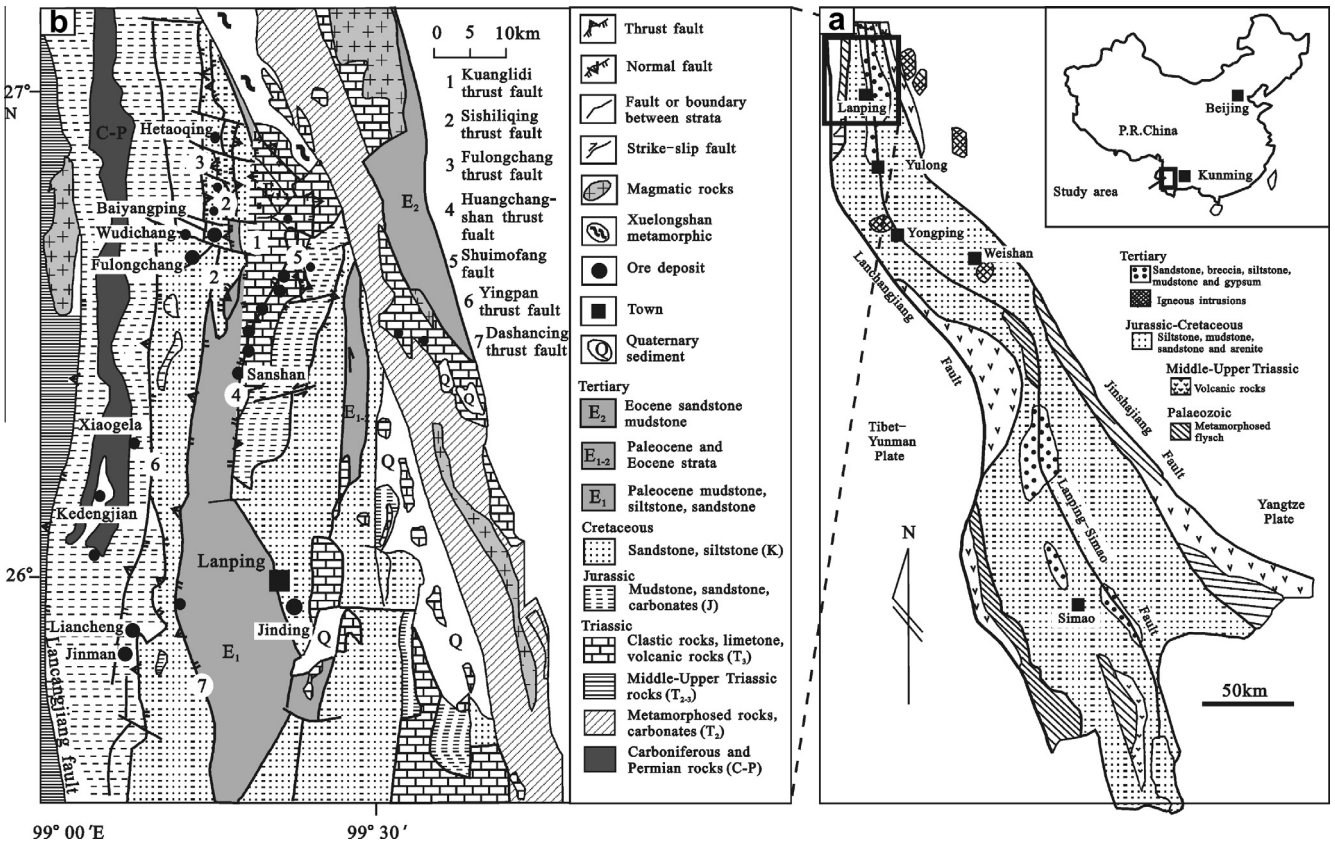

Fig. 1. (a) Sketch geological map of the Lanping–Simao foreland fold belt, China; (b) distribution map of main deposits in the northern Lanping basin (modified after Xue et al., 2007).

for these deposits, which hampers the identification of tectonic and geological events responsible for the mineralization, and fitting them into regional metallogeny (Li, 2001; Xue et al., 2003; Bi and Mo, 2004; He et al., 2004, 2009; Xu et al., 2004; Li and Song, 2006; Zhao, 2006; Wang, 2010). However, sediment-hosted base metal deposits are notoriously difficult to date, because most of them have simple mineral assemblages, and the associated host rock alteration is typically limited (e.g. Li and Fu, 2000; Xue et al., 2003, 2007; He et al., 2009). Moreover, no magmatic rock has been found either on the surface or underground in the mineralized areas, although Zhang et al. (2000) postulated a giant magmatic belt concealed beneath the northern Lanping basin.

We suggest that a comprehensive consideration of the ore-bearing horizon, the ore-controlling structure and isotopic chronological data is the key to accurately constrain the ages of these deposits. In this paper, we present and discuss new Re–Os dating result of molybdenite samples from the Liancheng deposit and Sm–Nd dating results of calcite samples from the Jinman deposit. We integrate these new data with previously published geochronological data and characteristics of the ore-controlling structure to review the mineralization ages of these typical deposits and constrain the metallogenic history of the Lanping basin by inference.

2. Geological setting of the Lanping basin

The Lanping–Simao foreland fold belt (Fig. 1a), a NNW-trending intra-continental basin, is located in the eastern Indo-Asian collision zone (EIACZ). This basin is clamped by the Jinshajiang–Ailaoshan suture to the east and the Lanchangjiang suture to the west (Fig. 1a; Xue et al., 2002, 2007; Hou et al., 2008; He et al., 2009). Tectonically, it is located at the border between Yangtze Plate to the east and the Tibet Plate to the west. The basement of the Lanping–Simao foreland fold belt consists primarily of Proterozoic and Palaeozoic strata (Xue et al., 2007; He et al., 2009). The Proterozoic metamorphic basement rocks (i.e. sericite schist, marble, gneiss) are distributed along the margins of the Lanping–Simao basin, and are similar to these of the Yangtze Plate (Mu et al., 1999; Xue et al., 2007).

The Lanping basin, as a part of the Lanping–Simao foreland fold belt, is filled with Mesozoic and Cenozoic strata to depths of more than 10 km (Fig. 1; Li and Fu, 2000; Xue et al., 2002, 2007). The Mesozoic and Cenozoic strata (Fig. 2) that outcrop in the Lanping basin are mainly composed of continental siliciclastic rocks, except for the lowest part of the sequence and the Upper Triassic Sanhedong Formation (T_3s), which mainly consist of marine limestone. The Mesozoic strata comprise the Upper Triassic Sanhedong Formation (T_3s) composed of marine carbonate rooks, the Middle Jurassic Hakaizuo Formation (J_2h) composed of carbonate-bearing sandstone and carbonaceous shale/slate; and the Lower Cretaceous Jingxing Formation (K_1j) composed of terrestrial red clastic rocks (Fig. 2; Mu et al., 1999; Xue et al., 2007). The Cenozoic strata are dominated by the Upper Paleocene Yunlong Formation (E_1y) composed of quartz sandstones and mudstones, and the Eocene Baoxiangsi Formation (E_2b) composed of pebbled sandstones (Fig. 2; Mu et al., 1999; Xue et al., 2007).

The outcrops of Himalayan magmatic rocks mostly occur along the margins of the Lanping basin. Only a few igneous rocks crop out inside the southern Lanping basin, including the Zhuopan and Huanglianpu intrusives in Yongping County, and the Weishan intrusive in Weishan County (Fig. 1; Xue et al., 2002, 2007). The petrologic types include quartz syenite, beschtauite,

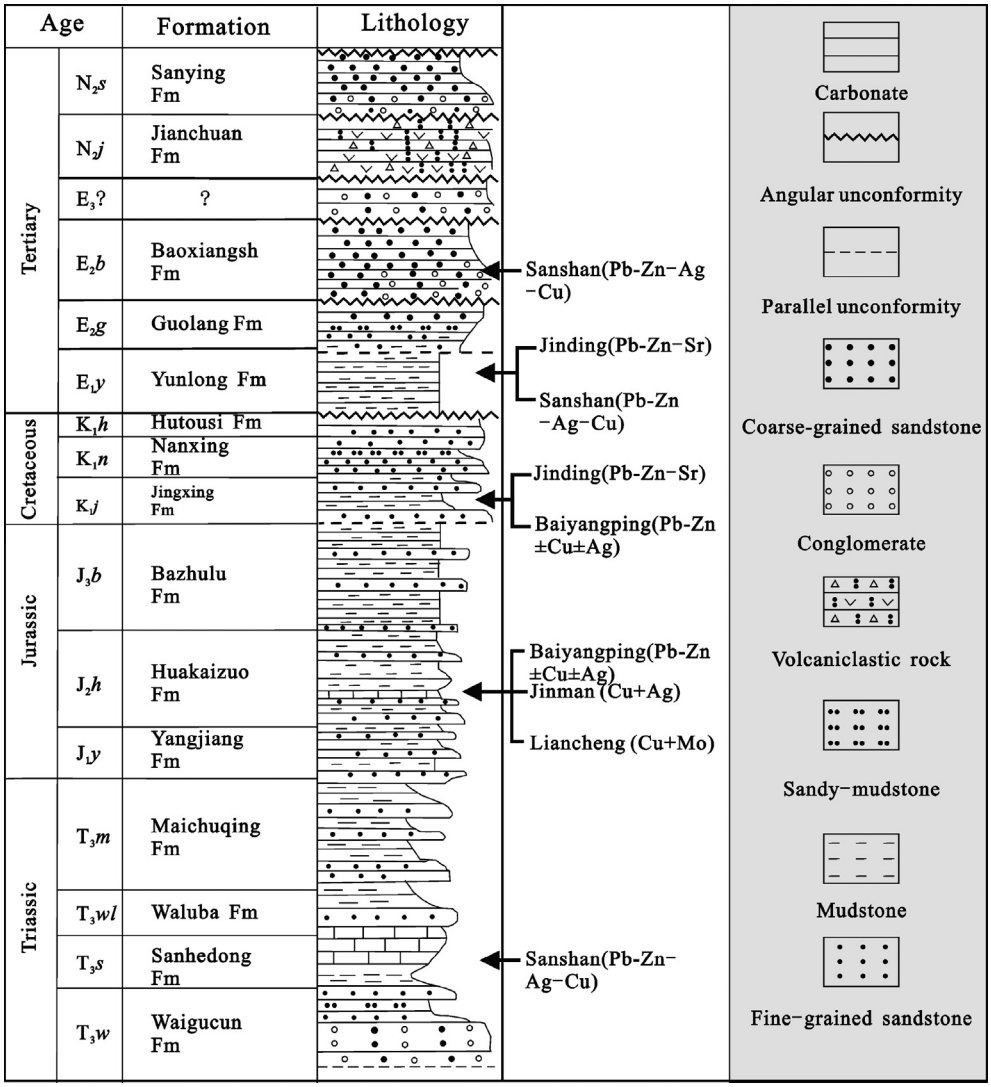

Fig. 2. An outline of the stratigraphic column in the Lanping basin (modified after Mu et al., 1999). Also shown are the stratigraphic positions of several typical deposits discussed in this study.

granite-porphyry, assyntite, and essexite, with ages ranging from 68 Ma to 23 Ma (Rb–Sr, U–Pb and Ar–Ar methods; Xue et al., 2003, 2007; Dong et al., 2005; Zhao, 2006). No magmatic rock occurs in the northern Lanping basin.

The dynamic process of the Lanping basin was jointly controlled by the trans-lithosphere faults along the basin margins and the penetrating-crust faults in the middle of this basin (Fig. 1, Zhang et al., 2000; Xue et al., 2002). The tectonic evolution of the Lanping basin was characterized by rifting in the Indo-Chinese epoch (rift basin), depression in the Yanshanian epoch (continental depression basin), and strike-slip extension in the Himalayan epoch (continental pull-apart basin) (Xue et al., 2002, 2007).

3. Distribution of the Pb–Zn–Cu–Ag deposits and related geology

As a consequence of the Indo-Asian collision (beginning at ~65 Ma; Hou et al., 2008), two large-scale Cenozoic thrust–nappe systems caused the thrusting of Mesozoic strata over the Tertiary strata in the Lanping basin, and dominated the spatial distribution of the Cenozoic Pb–Zn–Cu–Ag deposits (Hou et al., 2006; Xue et al., 2007; He et al., 2009). Over 100 thrust-controlled, sediment-hosted, Himalayan base metal deposits and mineral occurrences have been discovered in this basin, mostly located in the northern part (Fig. 1b; Hou et al., 2006; Xue et al., 2007; Khin et al., 2007; Hou et al., 2008; He et al., 2009). Spatially, the mineralization occurs in two sub-parallel metallogenic belts (Fig. 1b, Hou et al., 2006; He et al., 2009), divided by the central-axial fault. They are characterized by vein-type Cu polymetallic deposits in the western thrust–nappe system (e.g., the Jinman Cu deposit, the Liancheng Cu–Mo deposit and the Baiyangping Cu–Ag–Co deposit), and the Pb–Zn–Ag (±Cu) deposits in the eastern thrust–nappe system (e.g., the Jinding Zn–Pb deposit, the Sanshan Ag–Pb–Zn deposit) (Fig. 1b, Xue et al., 2007; Hou et al., 2008; He et al., 2009).

The geologic and mineralogical features of these typical deposits (Table 1) have been recently updated by Hou et al. (2008) and He et al. (2009). Features of several representative deposits are briefly summarized below.

3.1. The Jinding Pb–Zn deposit

The Jinding Pb–Zn deposit, controlled by the eastern thrust–nappe system, is the most important deposit in the eastern Lanping basin. This deposit (with a reserve of 200 Mt ore, grading 6.08% Zn

Table 1
Summary of geological and mineralogical features of economically significant deposits in the Lanping foreland fold belt.

Deposit	Structural location	Wall rock	Grade and tonnage	Sulfide assemblages	Economic metals	Data source
Jinding	The eastern thrust–nappe system	K_1j: sandstone and arenite; E_1y: breccia, sandstone and gypsum	Pb: 64 Mt; 1.16–2.42%, Zn: 12.84 Mt; 8.32–10.52%Ag: 1722 t; 12.5–12.6 g/t	Gn, Sp, Py, Mc, Cel, Sm	Zn–Pb	Xue et al. (2007)
Sanshan	The front zone of the eastern thrust–nappe system	T_3s: limestone and limestone; E_1y and E_2b: sandstone	Zn + Pb: 0.5 MtAg: 3000 tCu: ~0.3 Mt	Tet, Ar, Py, Az, Cp Sp, Gn	Ag–Pb–Zn–Cu	He et al. (2009)
Fulongchang	The front zone of the western thrust–nappe system	K_1j: sandstone and arenite; J_2h: quartz sandstone and mudstone	Ag: 2000 t, 328–547 g/t; Cu: 0.1 Mt, 0.63–11.70%; Pb: 4.2–7.4%	Tet, Py, Cp, Gn, Fre	Cu–Ag–Pb–Zn	Chen et al. (2000) and Zhao (2006)
Baiyangping	The front zone of the western thrust–nappe system	K_1j: sandstone and arenite; J_2h: quartz sandstone and mudstone	Ag: 3.0–33.8 g/t; Cu: 0.86–3.3%;Co: 0.10–0.27%	Tet, Py, Cp, Gn, Fre	Cu–Ag–Co	Chen et al. (2000) and Zhao (2006)
Jinman	The root zone of the western thrust–nappe system	J_2h: quartz sandstone, mudstone, carbonaceous shale, and slate	Cu:>0.2 Mt, 2.58%; minor Ag, ~100 g/t	Tet, Cp, Bo, Cc, Py	Cu–Ag	Li and Fu (2000) and Zhao (2006)
Liancheng	The root zone of the western thrust–nappe system	J_2h: quartz sandstone, mudstone, carbonaceous shale, and slate	Under exploration	Tet, Mo, Cp, Bo, Cc, Py	Cu–Mo	Li and Fu (2000) and Zhao (2006)

[a] *Ore mineral abbreviations*. Ar: argentite, Az: azurite, Bo: bornite, Cc: chalcocite, Cel: celestite, Cp: chalcopyrite, Fre: freibergite, Gn: galena, Mc: marcasite, Mo: Molybdenite, Py: pyrite, Sm: smithsonite, Sp: sphalerite, Tet: tetrahedrite.
[b] *Strata abbreviations*. E_2b: Eocene Baoxiangsi Formations; E_1y: Palaeocene Yunlong Formation; K_1j: Lower Cretaceous Jingxing Formation; J_2h: Middle Jurassic Huakaizuo Formation; T_3s: Upper Triassic Sanhedong Formation.

and 1.29% Pb) is the largest Pb–Zn deposit in China, and also the youngest sediment-hosted giant Pb–Zn deposit in the world (Xue et al., 2007; Khin et al., 2007).

The Jinding deposit occurs as tabular ore bodies and occasionally as lenses, veins or irregular shapes, in the fine sandstones of the Cretaceous Jingxing Formation (K_1j) and breccia-bearing sandstones of the Upper Paleocene Yunlong Formation (E_1y) near the Pijiang NS-trending fault (Fig. 3). The Jingxing Formation strata were thrust over the Yunlong Formation strata, and both the allochthonous and autochthonous strata are domed (the Jinding dome).

The ore bodies (Fig. 3) in the Jinding ore district are distributed around the core of the Jinding dome as "ring-shaped bodies", which is divided into six ore blocks (i.e. Beichang, Paomaping, Jiayashan, Xipo, Fengzishan, and Baicaoping) by a series of radial faults (Xue et al., 2007).

More than 30 primary minerals have been identified in the Jinding deposit. Ore minerals are dominated by sphalerite and galena, and some amounts of pyrite, chalcopyrite, argentite, and tetrahedrite are also present. Gangue minerals associated with mineralization include quartz, calcite, celestite, anhydrite, barite, and bitumen of various compositions (Xue et al., 2007). The deposit suffered from strong oxidization, forming a thick well-developed oxidized zone that accounts for 40% of the total reserve (Xue et al., 2007; He et al., 2009). Fluid inclusion and isotope data

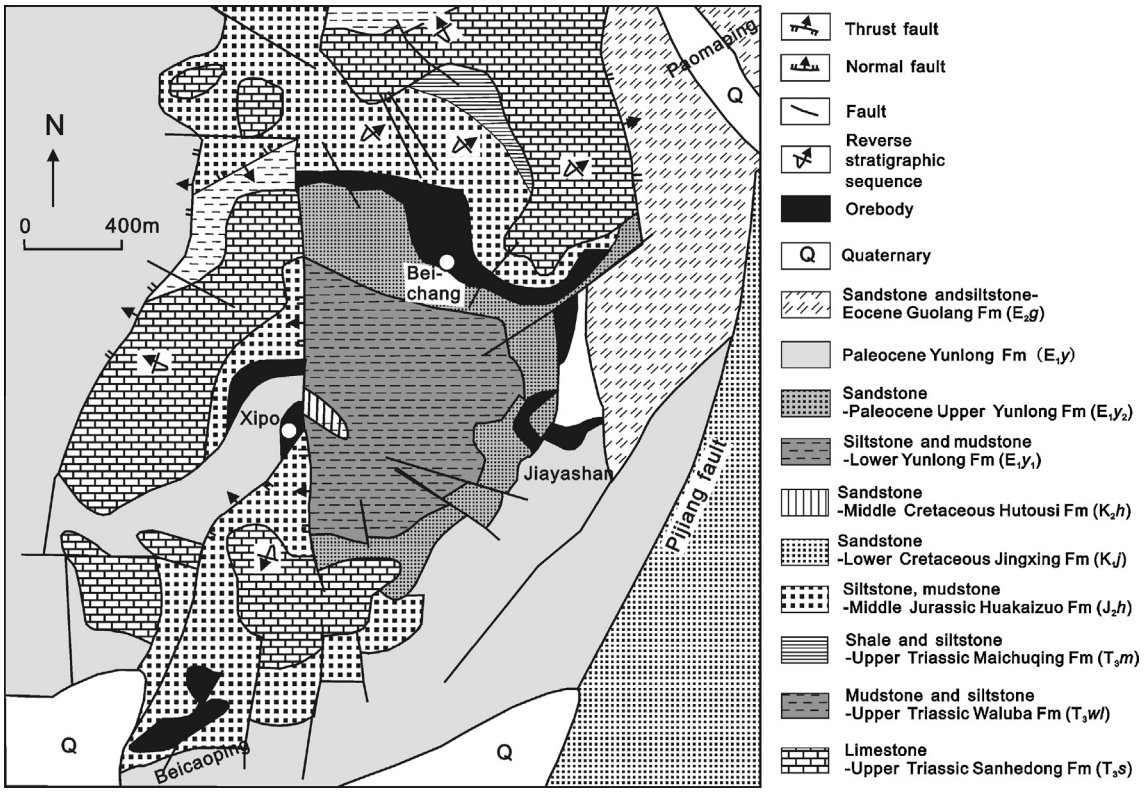

Fig. 3. Geological map of the Jinding Zn–Pb deposit in the Lanping basin (modified after Xue et al., 2007).

indicate that the hydrothermal fluid is a CO_2-bearing, low-temperature (mainly between 110 and 180 °C), low-salinity (1.6–18 wt.% NaCl equivalent) fluid, dominated by meteoric water, probably with a small proportion of mantle-sourced fluid (Zhao, 2006; Xue et al., 2007).

3.2. The Baiyangping Cu–Ag–Co ore belt

The Baiyangping Cu–Ag–Co ore belt (Fig. 4), consisting of two blocks (the Fulongchang and Baiyangping blocks), is an important deposit in the western Lanping basin. It is located in the front zone of the western thrust–nappe system in the western Lanping basin, about 30 km northwest of Jinding (Fig. 4). It has ~2000 t Ag, 0.12 Mt Cu, and minor reserves of Zn and Pb (Table 1). The ore bodies are mainly hosted in sandstones of the Cretaceous Jinxing Formation (K_1j), and partially in the siliceous mudstone of the Middle Jurassic Huakaizuo Formation (J_2h). The mineralization in the Baiyangping ore belt is dominated by open-space filling and cementation, and ore structures are dominated by veinlet, network and breccia structures.

Ore minerals are dominated by tetrahedrite, arsenian tetrahedrite, chalcopyrite, sphalerite, galena, argentite, and minor native silver (Zhao, 2006; He et al., 2009). Silver is mainly present as native silver, with minor amounts in tetrahedrite and argentite (Zhao, 2006). Gangue minerals include calcite, siderite, barite, and minor quartz (He et al., 2009). Fluid inclusion studies indicate that the ore-forming fluids for the Cu–Ag–Co mineralization are marked by low CO_2, low temperatures (mainly between 100 and 220 °C) and medium salinities (9.3–22.7 wt.% NaCl equivalent), and predominantly derived from basinal brines, recharged by meteoric water (He et al., 2009; Xue et al., 2010).

3.3. The Jinman Cu–Ag deposit

Jinman (Fig. 5a and c) is the largest and highest grade Cu deposit of the western metallogenic belt, located in the root zone of the western thrust–nappe system in the western Lanping basin (Fig. 1b). It has a reserve of 7.75 Mt ore with average grade of 2.58% Cu (under exploration), mainly hosted in Jurassic overturned strata (Hou et al., 2008; He et al., 2009). The deposit is controlled by a NNE-striking fault, which probably resulted from regional eastward thrusting (Hou et al., 2006). The main ore-hosted strata are a suite of terrestrial-marine low-grade metamorphic rocks composed of schists, sandy slates and mudstones of the Middle Jurassic Huakaizuo Formation. The wall rock alteration associated with mineralization is characterized by weak silicification and carbonatization, which mainly presents as siliceous rocks and veins of quartz, calcite, and dolomite, with minor siderite.

The ore bodies are dominated by sulfide-bearing quartz–calcite veins, although disseminated ore bodies in altered wall rocks are also common. The veins are generally parallel to bedding, with thicknesses ranging from tens of centimeters to a few millimeters (Fig. 6a–d).

Ore minerals are dominated by tetrahedrite, Ag-bearing tetrahedrite, chalcopyrite, bornite and chalcocite (Fig. 6a–d). Small amounts of pyrite, sphalerite, and galena are also present. Gangue minerals include quartz, calcite, ankerite, barite, and minor siderite and sericite (Liu et al., 2001; Hou et al., 2008; He et al., 2009).

On the basis of mineralization features, cross-cutting, and paragenetic relationships, the Jinman hydrothermal mineralization can be divided into three stages: (I) quartz + ankerite + minor chalcopyrite + tetrahedrite + minor pyrite stage, (II) quartz + syn-ore calcite + chalcopyrite + bornite + tetrahedrite + minor pyrite stage, and (III) quartz + post-ore calcite + minor chalcopyrite, chalcocite, covellite and bornite stage. Calcite, a common gangue mineral in this deposit, mainly occurs in the hydrothermal veins of the two latter stages (Fig. 6a–d). Based on field and microscopic observations, the calcite can be classified as either syn-ore or post-ore. Syn-ore calcite is usually intergrown with copper-bearing sulfides (e.g., chalcopyrite, bornite, and tetrahedrite), and is generally milky-white, locally yellowish-pink. Post-ore calcite is usually colorless and clear, coarse-grained, and appears in druses.

Fluid inclusion and isotope studies indicate that there are two fluid systems responsible for copper mineralization in the Jinman

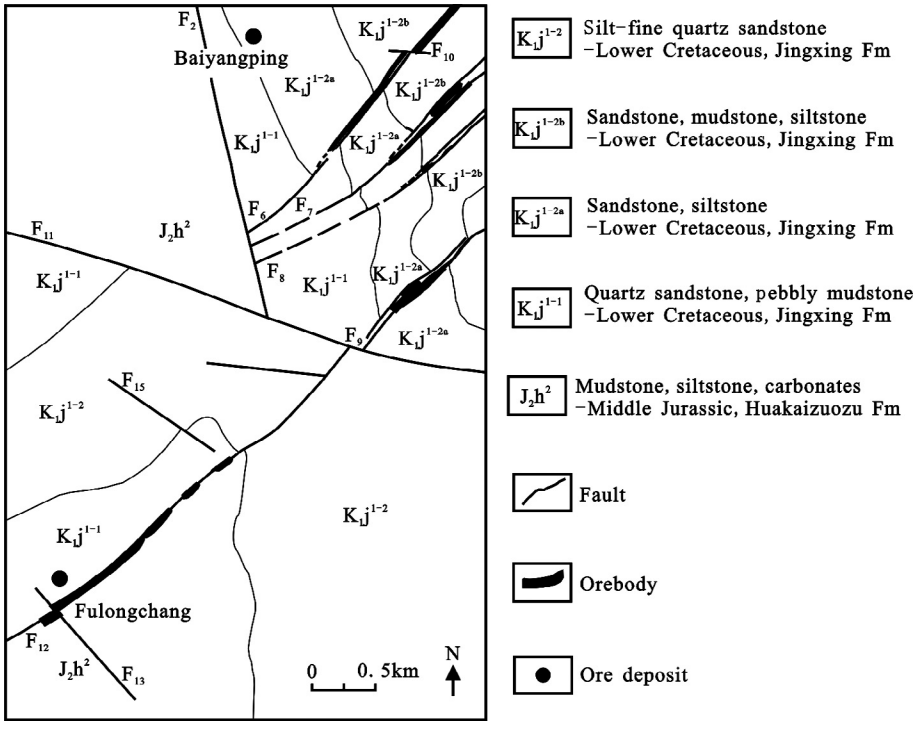

Fig. 4. Simplified geological map of the Fulongchang–Baiyangping deposit (modified from He et al., 2009).

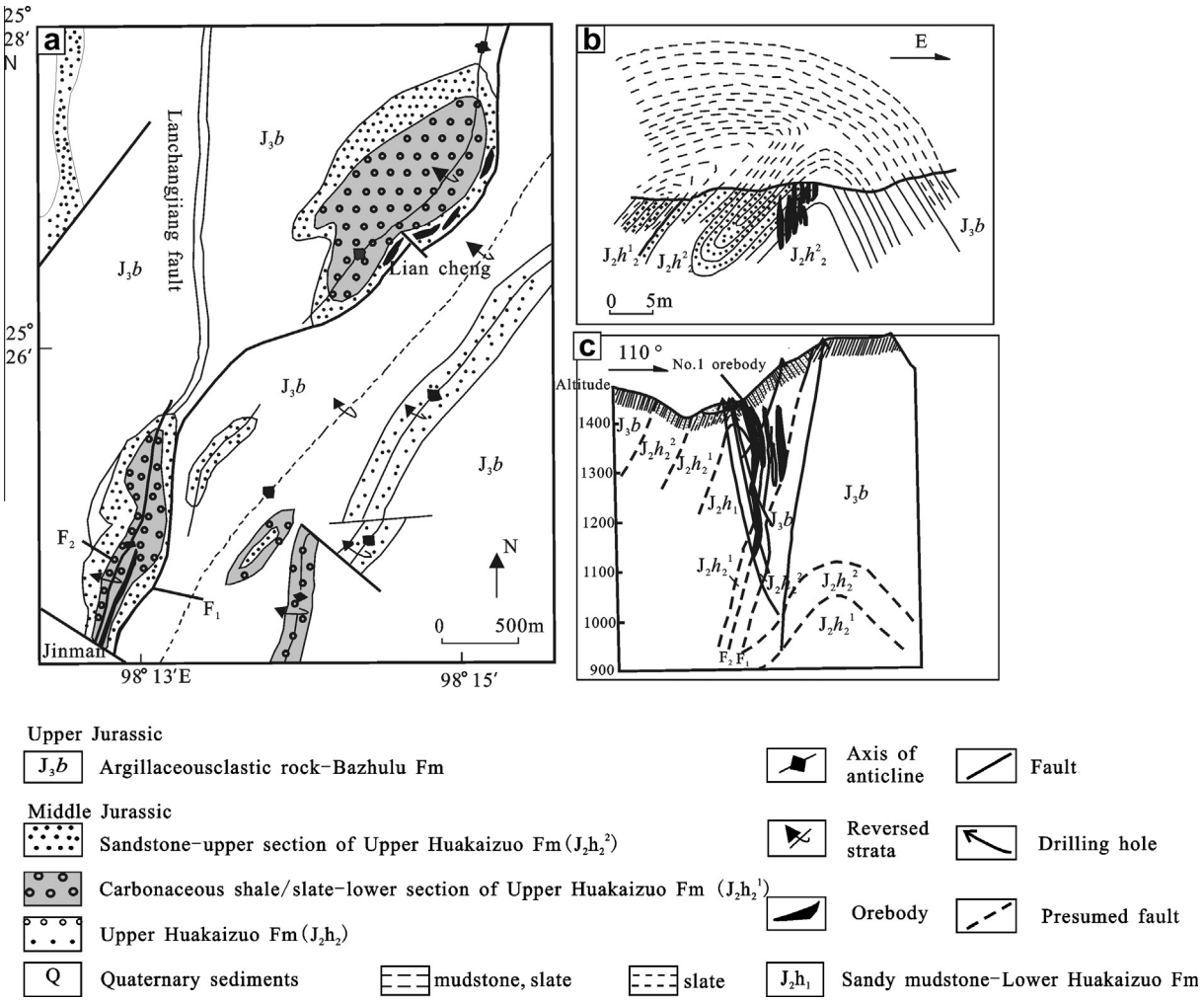

Fig. 5. (a) Geologic map of the Jinman and Liancheng deposits, (b) a cross-section through the orebody of the Liancheng deposit and, (c) a cross-section through the orebody of the Jinman deposit (modified from Li and Fu, 2000).

deposit. One is a deep derived fluid, characterized by high CO_2 content, relatively high temperatures (226–330 °C) and low salinities (1.6–13.4 wt.% NaCl equivalent), and the other is a basinal brine characterized by relatively high salinities (3.9–22.9 wt.% NaCl equivalent) and low temperatures (140–230 °C) (Ji and Li, 1998; Chi and Xue, 2011).

3.4. The Liancheng Cu–Mo deposit

The Liancheng Cu–Mo polymetallic deposit (Fig. 5a and b) is located in the root zone of the western thrust–nappe system (Fig. 1b), only ~2 km northwest of Jinman (Li and Fu, 2000). The ore bodies are mainly hosted in mottled elastic rocks, schist, sandy slates, and mudstones of the Middle Jurassic Huakaizuo Formation (Li and Fu, 2000; Zhao, 2006). The ore bodies in the deposit are mainly veins, with minor stratiform or lentiform bodies. Ore-bearing quartz and calcite vein systems are widespread in the Lancheng deposit, most of which occur parallel to the bedding of wall rock.

Ore minerals are dominated by tetrahedrite, chalcopyrite, molybdenite, bornite, and chalcocite, with minor pyrite. Gangue minerals include quartz, calcite, ankerite, and minor siderite (Li and Fu, 2000; Zhao, 2006). Based on paragenetic studies, the ore-forming process can be divided into early, middle, and late stages, characterized by quartz–molybdenite veins, quartz–copper sulfide veins, and carbonate veins, respectively (Fig. 6e–f; Li and Fu, 2000; Zhao, 2006; Zhang et al., 2012).

Hydrothermal fluids associated with the Cu–Mo mineralization are characterized by CO_2-rich, high temperature (177–346 °C) and moderate salinity (2–4 wt.% NaCl and 8–18 wt.% NaCl equivalent; Zhao, 2006; Zhang et al., 2012). The $\delta_{18}O$ values of the ore-forming fluid range from 5.5‰ to 8.6‰ and the corresponding δD values range from −56‰ to −109‰, suggesting that the mineralizing fluids are dominated by magmatic water, with a small proportion of meteoric water (Zhao, 2006; Zhang et al., 2012).

4. Sample description and analytical methods

4.1. Sampling details

Based on field textural features and microscopic observation, nine representative calcites that coexisted with copper-bearing sulfides were selected for analysis (Fig. 6a–d). These calcite samples were collected from quartz and calcite veins with tetrahedrite, chalcopyrite, and minor pyrite (Fig. 6a and b), that crosscut the pre-ore quartz and ankerite veins. These ore-bearing quartz and calcite veins are from the No.3 mine in the Jinman deposit at 1230 m altitude. The samples were crushed, sieved and hand-picked under a binocular microscope to a purity of more than 99%, and finally ground as fine as 200 meshes in size with an agate mortar.

Five representative molybdenite samples from the Liancheng Cu–Mo deposit were collected for analysis. These molybdenite

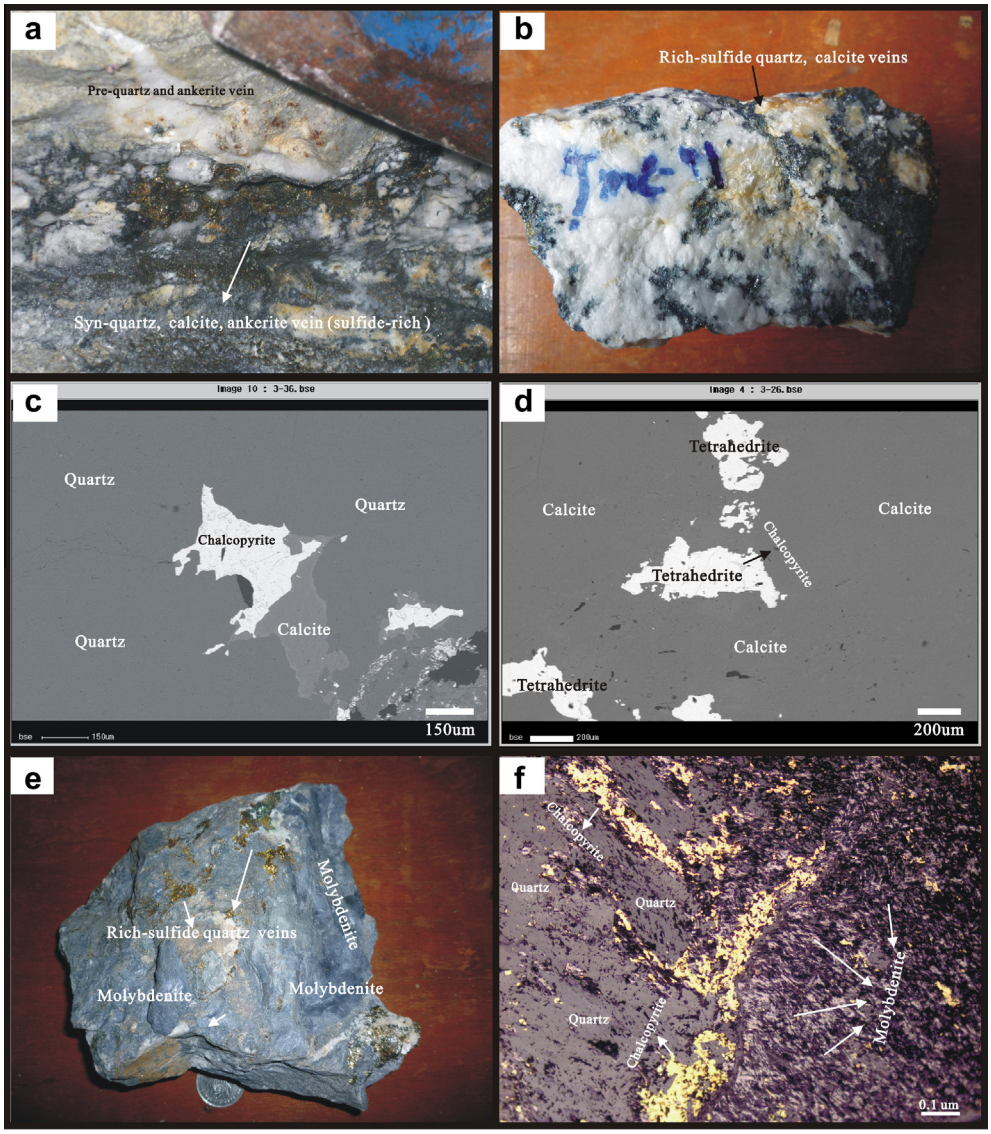

Fig. 6. Scanned pictures of ores and photomicrographs showing relationships of hydrothermal minerals in the Jinman and Liancheng deposits. (a) Syn-ore quartz and calcite veins (bearing some copper sulfides) cutting pre-ore quartz and vein. (b) Sulfide-rich quartz and calcite veinlets. (c) EMPA back-scattered electron (BSE) image of the quartz that was cut by some chalcopyrite-bearing quartz veinlets. (d) EMPA back-scattered electron (BSE) image of chalcopyrite, and tetrahedrite in the syn-ore calcite. (e) Early molybdenite penetrated by quartz-sulfide veins. (f) Early fibrous molybdenite penetrated by quartz-sulfide vein.

samples (Fig. 6e and f) were collected from sulfide-quartz veins with molybdenite, chalcopyrite, and minor pyrite filling fractures of the altered host rock. These ore-bearing quartz veins were from the No.2 mine in the Liancheng deposit. The molybdenite samples were handpicked under a binocular microscope to remove all impurities, and then milled to powder with an agate mortar.

4.2. Sm–Nd geochronology of calcite

The calcite samples were analyzed on a MAT-261 mass spectrometer at Tianjin Institute of Geology and Mineral Resources, the Chinese Academy of Geological Sciences (CAGS). The isotope composition of Nd was normalized to $^{146}Nd/^{144}Nd = 0.7219$. The reproducibility of the isotopic ratios is better than 0.005% at the 2-sigma-mean level (2σ-mean); the precision for Sm and Nd concentrations is less than 0.5% (2σ). The average concentrations and Nd isotope ratio for BCR-1 measured in this work were 6.57 ppm for Sm, 28.75 ppm for Nd and 0.512644 ± 5 (2σ, $n = 6$) for $^{143}Nd/^{144}Nd$, in accordance with the literature values of 6.58 ppm for Sm and 28.8 ppm for Nd (Bell et al., 1989; Peng et al., 2003; Su et al., 2009). The JMC calcite standard (the Johnson and Mattey® Nd standard) gave an average $^{143}Nd/^{144}Nd$ value in the range of 0.511132 ± 5 (2σ). Average blanks in this work were 0.03 ng for Sm and 0.05 ng for Nd. The decay constant used in the age calculation is $\lambda^{147}Sm = 6.54 \times 10^{-12}$/yr. The Sm–Nd isochron ages were calculated with ISOPLOT 2.9 (Ludwig, 1996). Additional details of analytical procedures can be found in Peng et al. (2003) and Su et al. (2009).

4.3. Re–Os geochronology of molybdenite

The molybdenite samples were analyzed using a TJA Plasmaquad ExCell inductively coupled plasma-mass spectrometry (ICP-MS) at the Re–Os Lab, National Research Center of Geoanalysis, Chinese Academy of Geological Sciences in Beijing.

Average blanks for the total Carius tube procedure were approximately 5 pg Re and 2 pg Os. The analytical results were inspected by repeated analyses of the JDC molybdenite standard. The

uncertainty in each individual age determination is about 1.4%, including the uncertainty of the decay constant of ^{187}Re, uncertainty in the isotope ratio measurement, and spike calibrations. The average Re–Os age of the JDC standard is 139.5 ± 1.9 Ma (95% confidence level). The average Re and Os concentrations are 17.3 ± 0.1 μg/g and 25.2 ± 0.2 ng/g, respectively. The JDC standard age and Os and Re contents in this study are in agreement with results reported by Du et al. (2004).

A decoupling effect in the Re–Os molybdenite system has recently been noticed (Kosler et al., 2003; Stein et al., 2003; Selby and Creaser, 2004; Du et al., 2007). Selby and Creaser (2004) and Du et al. (2007) pointed out that efficiently overcoming this decoupling effect is crucial for obtaining accurate and reproducible Re–Os molybdenite dates, and fine-grained (<2 mm) molybdenite appears to show little decoupling. The molybdenite in the Liancheng deposit occurs mainly as fine- and micro-grained particles, which are suitable for Re–Os isotopic dating. The decay constant used in the age calculation is $\lambda^{187}\mathrm{Re} = 1.666 \times 10^{-11}$/yr (Smoliar et al., 1996). The Re–Os isochron ages were calculated with ISOPLOT 2.9 (Ludwig, 1996). Additional details of analytical procedures have been described by Du et al. (1994, 2004), Shirey and Walker (1995), and Mao et al. (2008).

5. Results

5.1. Sm–Nd geochronology of calcite in the Jinman Cu–Ag deposit

Concentrations of Sm and Nd for calcite samples and their isotope compositions are reported in Table 2, and presented on the ^{147}Sm/^{144}Nd–^{143}Nd/^{144}Nd diagrams (Fig. 7). As shown in Table 2, the ^{147}Sm/^{144}Nd values range from 0.1323 to 0.3856, with corresponding ^{143}Nd/^{144}Nd values between 0.512179 and 0.512274. On the ^{147}Sm/^{144}Nd–^{143}Nd/^{144}Nd diagrams, the nine calcite samples plot along a linear array (Fig. 6), which may reflect an isochron or a mixing line of two end-members having different ^{147}Sm/^{144}Nd and ^{143}Nd/^{144}Nd ratios (Jiang et al., 2000; Peng et al., 2003). The nonlinear relationship existing on the 1/Nd–^{143}Nd/^{144}Nd diagrams for calcites excludes the possibility of a mixing line (Fig. 8). The calcite yields an age of 58.2 ± 5.3 Ma (2σ), with an intercept of 0.5121285 ± 74 (initial ε_{Nd} = –8.4). The mean square of weighted deviates (MSWD) is 0.039. Significantly, the MSWD here is abnormally low, which may be due to overestimated analytical errors (Peng et al., 2003; Su et al., 2009).

5.2. Re–Os geochronology of molybdenite in the Liancheng Cu–Mo deposit

The five molybdenite samples from the Liancheng deposit yield similar model ages, ranging from 51.0 ± 0.8 to 48.4 ± 0.9 Ma (2σ) (Table 3), although their ^{187}Re and ^{187}Os contents vary in a wide range.

The five samples plot along a linear array on the isochron diagram (Fig. 9), and the isochron age calculated with the ISOPLOT software is 47.8 ± 1.8 Ma (2σ), with an initial ^{187}Os value (ng/g) of 0.8 ± 1.1 (MSWD = 7.2).

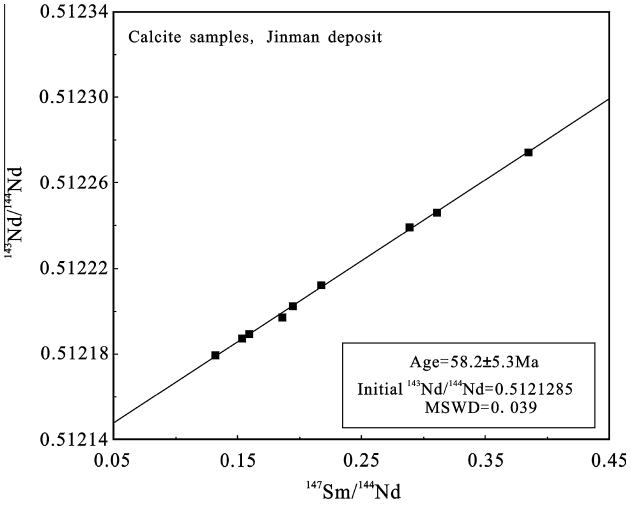

Fig. 7. The Sm–Nd isochron for calcites from the Jinman deposit.

6. Discussion

The data presented herein, combined with those compiled from previous studies (Tables 3 and 4; e.g. Xue et al., 2003; Bi and Mo, 2004; He et al., 2004; Zhao, 2006; Wang et al., 2011) show that isotope chronological data of the Cu–Ag polymetallic mineralization in the western Lanping basin cluster into three age groups: 58–54, 51–48 and 31–29 Ma, and the Pb–Zn–Ag (±Cu) polymetallic mineralization in the eastern Lanping basin cluster into ages of 72–68, 56 and 32–20 Ma. However, accurate timing and duration of the Pb–Zn–Cu–Ag mineralization in the Lanping basin are still widely controversial, because of the different geological interpretations of these ages (Xue et al., 2003, 2007; Hou et al., 2006; Zhao, 2006; He et al., 2009). Moreover, some age data are geologically implausible and contradict the basic geological features of these deposits, as discussed in what follows. As a result, we suggest that a comprehensive consideration of ore-bearing horizon, ore-controlling structure and isotope chronologic data is the key to accurately constrain the ages of these deposits. The mineralization ages of the Cu–Ag and Pb–Zn–Ag (±Cu) polymetallic deposits are discussed in more detail below.

6.1. Ages of western thrust-controlled Cenozoic Cu–Ag polymetallic deposits

A series of Cu–Ag polymetallic deposits controlled by the western thrust-nappe system and secondary structures occur in the northwestern Lanping basin, including the Jinman Cu deposit, the Liancheng Cu–Mo deposit, and the Baiyangping Cu–Ag–Co ore belt

Table 2
Sm and Nd isotope composition for calcites associated with sulfides from the Jinman deposit.

Sample no.	Analyzed phase	Sm/ppm	Nd/ppm	^{147}Sm/^{144}Nd	^{143}Nd/^{144}Nd (2σ-mean)
JM-3	Calcite	9.70	20.29	0.2892	0.512239 ± 10
JM-6	Calcite	3.83	6.00	0.3856	0.512274 ± 48
JM-17	Calcite	7.01	13.60	0.3116	0.512246 ± 21
JM-40	Calcite	4.88	18.45	0.1599	0.512189 ± 36
JM-41	Calcite	5.87	18.20	0.1950	0.512202 ± 11
JM-43	Calcite	6.95	19.28	0.2180	0.512212 ± 11
JMC-1	Calcite	15.91	62.61	0.1536	0.512187 ± 19
JMC-4	Calcite	27.31	88.44	0.1867	0.512197 ± 32
09JM-10	Calcite	9.60	43.87	0.1323	0.512179 ± 8

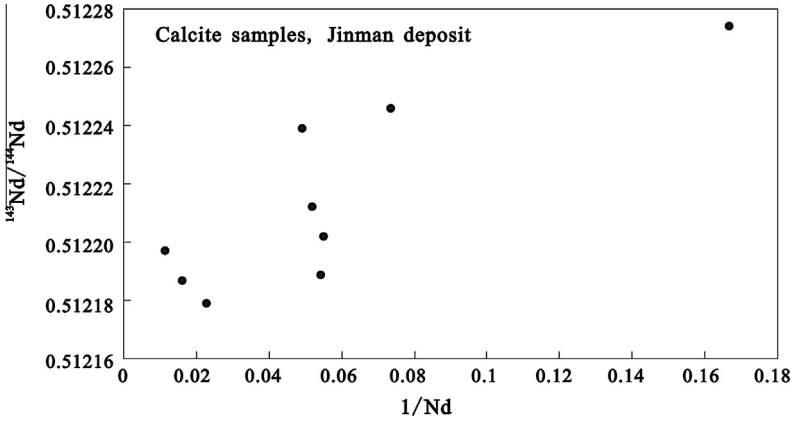

Fig. 8. The 1/Nd vs. $^{143}Nd/^{144}Nd$ plot for the calcites from the Jinman deposit.

Table 3
Re and Os isotope composition for molybdenite from the Liancheng deposit.

Sample no.	Analyzed phase	Total Re (ppm)	^{187}Re (ppm)	^{187}Os (ppb)	Model age (Ma)
LC11-11	Molybdenite	159.0 (2.2)	99.9 (1.4)	80.6 (0.7)	48.4 (0.9)
LC03-4	Molybdenite	51.2 (0.4)	32.2 (0.3)	26.8 (0.2)	49.9 (0.7)
LC02-1	Molybdenite	32.9 (0.3)	20.7 (0.2)	17.6 (0.2)	51.0 (0.8)
09EN-7	Molybdenite	28.3 (0.3)	17.8 (0.2)	14.8 (0.1)	49.8 (0.8)
LC11-14	Molybdenite	62.2 (0.6)	39.1 (0.4)	31.6 (0.3)	48.4 (0.7)

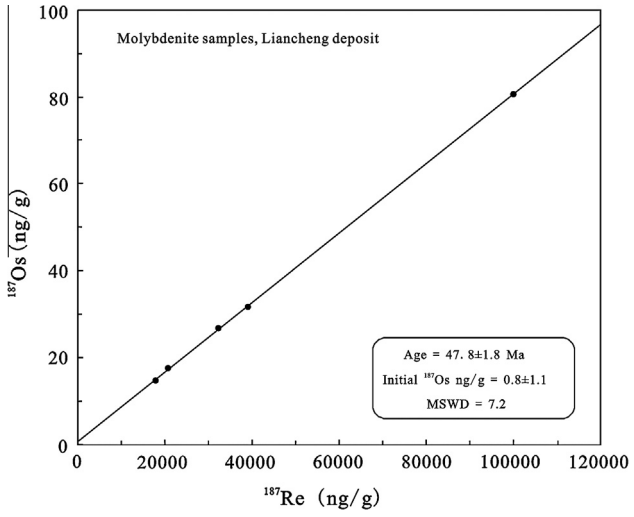

Fig. 9. The Re–Os isochron for molybdenites from the Liancheng deposit.

(Fig. 2 and Table 1; Chen et al., 2000, 2004; Zhao, 2006; Hou et al., 2006; He et al., 2009). Thus, the mineralization should occur during or immediately after thrust–nappe deformation in the western Lanping basin, and definitely after deposition of the strata involved in the system (Zhao, 2006; He et al., 2009).

The Upper Paleocene Yunlong Formation (E_1y) is regionally involved in the western thrust–nappe system, and is unconformably overlain by Eocene strata (Fig. 2; Xue et al., 2007; Wang, 2010). Therefore, the Cu–Ag polymetallic mineralization should postdate the deposition of the Yunlong Formation (E_1y) (ca. 56 Ma at the end of the Paleocene; Mu et al., 1999; He et al., 2009; Wang, 2010).

At Jinman, the correlation coefficient for the Rb–Sr isochron age of the fluid inclusions in quartz (66.8 Ma, Li, 2001) is low (0.776) and, thus, most likely represents an "errorchron". In addition, Xu et al. (2004) analyzed quartz coexisting with copper-bearing sulfide from the Jinman deposit using the ^{40}Ar–^{39}Ar fast-neutron activation dating technique, and acquired a well-defined plateau age of 56.7 ± 1.0 Ma and an isochron age of 56.8 ± 0.7 Ma. With the same dating method, Liu et al. (2003) acquired a plateau age of 58.1 ± 0.5 Ma and an isochron age of 54.3 ± 0.1 Ma on similar quartz samples. Considering that the quartz samples coexist with copper-bearing sulfide and their ages are consistent, we believe that these ages are reliable. These ^{40}Ar–^{39}Ar ages are nearly identical to the Sm–Nd isochron age obtained in this study. Therefore, we suggest that these two sets of age data are reliable and represent the main mineralization age of the Jinman Cu–Ag deposit. The younger sericite Ar–Ar age (36.8 ± 0.8 Ma; Wang et al., 2005) and conventional K–Ar ages (47.2–35.4 Ma; Bi and Mo, 2004; Zhao, 2006) on hydrothermal illite from the altered wall rocks can be interpreted as the age of late hydrothermal activity. These ages are consistent with emplacement of the Cenozoic alkaline intrusive rocks in the Lanping basin (e.g. Zhuopan intrusive, Huanglianpu intrusive, and Weishan intrusive; with Ar–Ar ages of 46.5 Ma, 36.7 Ma, and 38.8 Ma, Dong et al., 2005).

These radiometric age data (Table 4), combined with ore-controlling structure and ore–bearing horizon information (Table 1), indicate that the main Cu–Ag mineralization of the Jinman deposit took place at ca. 56–54 Ma, corresponding to the main-collisional stage of the Indo-Asian collision orogeny (Hou et al., 2006, 2007). Possibly, there was a remobilization or a new phase of Cu mineralization in the duration from 35 to 47 Ma.

In the Liancheng deposit, the molybdenite Re–Os isochron age (47.8 ± 1.8 Ma) is consistent with the model ages (51.0 ± 0.8 to 48.4 ± 0.9 Ma) within the error limits, although the MSWD of 7.2 is slightly high. The most plausible explanation is that the mineralization in the Liancheng Cu–Mo deposit happened within the duration from 51 to 48 Ma, which corresponds to the main-collisional stage of the Indo-Asian collision orogeny (Hou et al., 2006, 2007).

Quartz ^{40}Ar–^{39}Ar dating from the Baiyangping Cu–Ag–Co ore belt gave an age of 56.5 ± 0.4 Ma (He et al., 2004). However, this age is geologically implausible, because the mineralization partly occurs within the Upper Paleocene strata (E_1y). Moreover, a detailed field investigation (Zhao, 2006) revealed that only a few

Table 4
Summary of age data of the economically significant deposits in the Lanping foreland fold belt.

Ore belt	Deposit	Economic metal	Analyzed phase	Method	Age (Ma)	Reference
West	Jinman	Cu, Ag	Fluid inclusions in quartz intergrown with Cu-bearing sulfide	^{40}Ar–^{39}Ar	54.3 ± 0.2	Liu et al. (2003)
West	Jinman	Cu, Ag	Fluid inclusions in quartz intergrown with Cu-bearing sulfide	^{40}Ar–^{39}Ar	56.8 ± 0.7	Xu et al. (2004)
West	Jinman	Cu, Ag	Sericite from altered wall rock	^{40}Ar–^{39}Ar	36.8 ± 0.8	Wang et al. (2005)
West	Jinman	Cu, Ag	Illite from altered wall rock	K/Ar	46.7 ± 0.7	Bi and Mo (2004)
West	Jinman	Cu, Ag	Illite from altered wall rock	K/Ar	47.2 ± 0.5 37.0 ± 0.4 35.4 ± 0.3 41.0 ± 0.3	Zhao (2006)
West	Jinman	Cu, Ag	Calcite intergrown with Cu-bearing sulfide	Sm–Nd	58.2 ± 5.3	This study
West	Liancheng	Cu, Mo	Molybdenite	Re–Os	48.7 ± 1.8	This study
West	Baiyangping	Cu, Ag, Pb, Zn	Fluid inclusions in quartz	^{40}Ar–^{40}Ar	56.5 ± 0.4	He et al. (2004)
West	Baiyangping	Cu, Ag, Pb, Zn	Calcite	Sm–Nd	29.9 ± 1.1	Wang et al. (2011)
West	Baiyangping	Cu, Ag, Pb, Zn	Sphalerite	Rb–Sr	28.9 ± 0.6	Wang et al. (2011)
East	Jinding	Pb, Zn, Sr	Pyrite from Jinding ore district	Re–Os	72 ± 4	Xue et al. (2003)
East	Jinding	Pb, Zn, Sr	Bitumen from Jinding ore district	Re–Os	68 ± 5	Wang et al. (2011)
East	Jinding	Pb, Zn, Sr	Apatite from orebody bottom	Fission track	28.7 ± 2.8	Li and Song (2006)
East	Jinding	Pb, Zn, Sr	Apatite from eastern orebody	Fission track	21.0 ± 3.8	Li and Song (2006)
East	Jinding	Pb, Zn, Sr	Apatite from orebody roof	Fission track	32.1 ± 5.1	Li and Song (2006)
East	Sanshan	Pb, Zn, Ag, Cu	Apatite from orebody	Fission track	19.9 ± 2.3	Li and Song (2006)

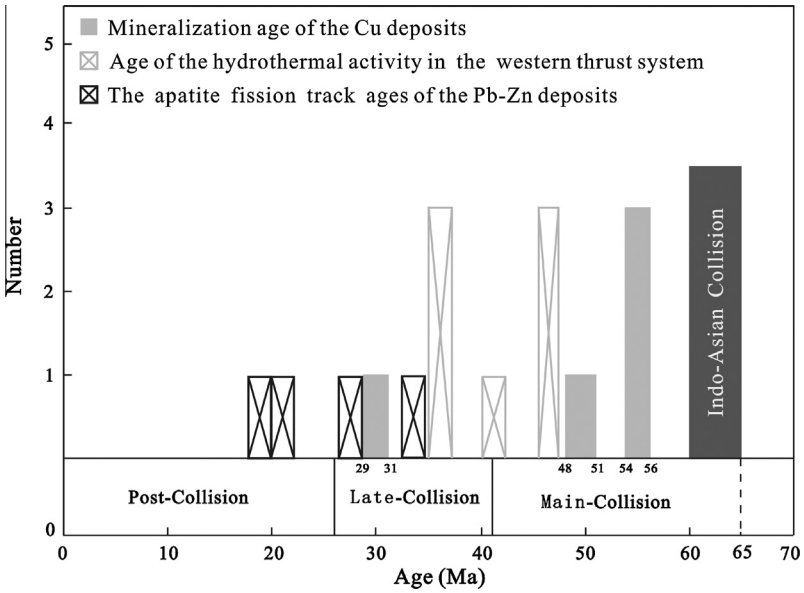

Fig. 10. The relationship between the episodic mineralization events and the overall geodynamic setting in the eastern Indo-Asian collision zone.

quartz veins occurred in the Baiyangping ore belt, which showed no genetic relationship with mineralization. Thus, it is possible that the dated quartz samples from Baiyangping are protoliths.

Possibly, the Sm–Nd isochron age data (29.9 ± 1.1 Ma) on ore-bearing calcite and the Rb–Sr isochron age (28.9 ± 0.6 Ma) of coexisting sphalerite reported by Wang et al. (2011) from the Baiyangping ore belt can be interpreted as the main mineralization age, roughly corresponding to the late-collisional stage of the Indo-Asian collision orogeny (Fig. 10, Hou et al., 2006, 2007).

6.2. Ages of eastern thrust-controlled Cenozoic Pb–Zn–Ag (± Cu) deposits

Controlled by the eastern thrust-nappe system, a large number of epithermal Pb–Zn–Ag (±Cu) deposits occur in the eastern Lanping basin, including the giant Jinding Pb–Zn, and Sanshan Ag–Pb–Zn deposits (Table 1; Chen et al., 2000; Hou et al., 2006; He et al., 2009). Comprehensive geochronological studies of these Pb–Zn–Ag (±Cu) deposits, using Re–Os and apatite fission track methods, were published by Xue et al. (2003), Li and Song (2006), and Gao et al. (2012). Ore pyrite from the giant Jinding deposit gave an age of 72 ± 4 Ma using the Re–Os method (Xue et al., 2003). Bitumen hosted in the breccia-bearing sandstones of the Upper PaleoceneYunlong Formation in the Jinding deposit gave a Re–Os isochron age of 68 ± 5 Ma (MSWD = 9.2, n = 6; Gao et al., 2012). However, these ages are geologically implausible because the mineralization of these deposits partially occurs within the Paleocene (E_1y) and Upper Eocene strata (E_2b) (Table 1; Xue et al., 2007; He et al., 2009). Moreover, the Pb–Zn–Ag (±Cu) deposits are controlled by the eastern thrust–nappe system and its secondary structures (Hou et al., 2006; Xue et al., 2007; He et al., 2009). Therefore, the mineralization should postdate thrusting in the eastern Lanping basin, and certainly postdate the strata involved in the thrust–nappe system. The Upper Eocene Baoxiangsi Formation (E_2b) stratum is regionally involved in the eastern thrust-nappe system, which is unconformably overlain by Oligocene strata (Fig. 2; Mu et al., 1999; He et al., 2009; Wang, 2010). This suggests that the mineralization probably happened after deposition of the E_2b stratum (~37 Ma; Zhao, 2006; He et al., 2009).

As has been discussed, the accurate timing and duration of the Pb–Zn–Ag (±Cu) mineralization in the eastern Lanping basin still remain as unsolved problems. However, the age data (21.0 ± 3.8 Ma to 32.1 ± 5.1 Ma, apatite fission track method) reported by Li and Song (2006) may suggest some constraints on the mineralization ages of these Pb–Zn–Ag (±Cu) deposits (Fig. 10). Generally, apatite fission track ages could be related to any thermal event in such an orogenic context. However, the apatite samples are taken from the ore bodies of these Pb–Zn–Ag (±Cu) deposits in the eastern Lanping basin, and the closure temperature of apatite fission tracks (~110 °C) (Li and Song, 2006) is close to the mineralization temperatures of these deposits (mainly between 110 and 180 °C; Zhao, 2006; Xue et al., 2007). Therefore, we suggest that these fission track ages possibly represent the mineralization ages, at least for the periods of hydrothermal activity.

On the basis of a comprehensive consideration of ore-bearing horizon, ore-controlling structure, and isotope chronological data, we propose that: (1) the main metallogenic stages of Cu–Ag mineralization in the western Lanping basin are at ca. 56–54, 51–48, and 31–29 Ma, corresponding to the main- and late-collisional stages of the Indo-Asian collision orogeny. A Cu remobilization or a new phase of Cu mineralization in the Jinman deposit is posited from 35 to 47 Ma, because K–Ar and ^{40}Ar–^{39}Ar ages show significant hydrothermal activity at that time (Fig. 10); and (2) although the Pb–Zn–Ag (±Cu) mineralization in the eastern Lanping basin has not been dated directly with precision, apatite fission track ages (21.0 ± 3.8 Ma to 32.1 ± 5.1 Ma, corresponding to the late-collisional stage of the Indo-Asian collision orogeny), offer a possible constraint.

7. Conclusions

1. The Cu–Ag mineralization in the western Lanping basin mainly occurs in three episodes (i.e., ~56–54, 48, and 31–29 Ma), corresponding to the main- and late-collisional stages of the Indo-Asian collision orogeny.
2. The mineralization ages of Pb–Zn–Ag (±Cu) deposits controlled by the eastern thrust–nappe system are probably younger than 37 Ma, possibly corresponding to the late-collisional stage of the Indo-Asian collision orogeny. However, more work is necessary to precisely constrain the ages of ore deposits in the eastern Lanping basin.
3. The main Cu–Ag mineralization controlled by the western thrust–nappe system in the western Lanping basin probably predates the Pb–Zn–Ag (±Cu) mineralization in the eastern Lanping basin.

Acknowledgements

This work was financially supported by the National Basic Research Program of China (No. 2009CB421005), the 12th Five-Year Plan project of State Key Laboratory of Ore-deposit Geochemistry, Chinese Academy of Sciences (SKLODG-ZY125-07), and National Natural Science Foundation of China (Grant Nos. 40930425 and 41173026). We are grateful to the geologists from the Sanjiang Copper Company Limited for their assistance during our field investigation. Mrs. Hui Liu of Tianjin Institute of Geology and Mineral Resources is greatly appreciated for her help with analyses and technical assistance in the Sm–Nd isotope analysis.

References

Bell, K., Anglin, C.D., Franklin, J.M., 1989. Sm–Nd and Rb–Sr isotope systematics of scheelites: possible implications for the age and genesis of vein-hosted gold deposits. Geology 17, 500–504.

Bi, X.M., Mo, X.X., 2004. Transition from diagenesis to low-grade metamorphism and related minerals and energy resources. Earth Sciences Frontiers 11, 287–294 (in Chinese with English).

Chi, G.X., Xue, C.J., 2011. Abundance of CO_2-rich fluid inclusions in a sedimentary basin-hosted Cu deposit at Jinman, Yunnan, China: implications for mineralization environment and classification of the deposit. Mineralium Deposita 46, 365–380.

Chen, K.X., He, L.Q., Yang, Z.Q., Wei, J.Q., Yang, A.P., 2000. Oxygen and carbon isotope geochemistry in Sanshan–Baiyangping copper–silver polymetallic enrichment district, Lanping, Yunnan. Geology and Mineral Resources of South China 4, 1–8 (in Chinese with English abstract).

Chen, K.X., Yao, S.Z., He, L.Q., Wei, J.Q., Yang, A.P., Huang, H.L., 2004. Ore-forming fluid of the Baiyangping silver-polymetallic mineralization concentration field in the Lanping basin, Yunnan Province. Geological Science and Technology Information 23, 45–50 (in Chinese with English abstract).

Dong, F.L., Mo, X.X., Hou, Z.Q., Wang, Y., Bi, X.M., Zhou, S., 2005. $^{40}Ar/^{39}Ar$ ages of Himalayan alkaline rocks in the Lanping basin, Yunnan and their geological significance. Acta Petrologica Mineralogica 24, 103–109 (in Chinese with English abstract).

Du, A.D., He, H.L., Yin, W.N., 1994. The study on the analytical methods of Re–Os age for molybdenite. Acta Geologica Sinica 68, 339–346 (in Chinese with English abstract).

Du, A.D., Wu, S.Q., Sun, D.Z., Wang, S.X., Qu, W.J., Markey, R., Stein, H., Morgan, J.W., Malinovskiy, D., 2004. Preparation and certification of Re–Os dating reference materials: molybdenite HLP and JDC. Geostandard and Geoanalytical Research 28, 41–52.

Du, A.D., Qu, W.J., Wang, D.H., Li, H.M., Feng, C.Y., Liu, H., Ren, J., Zeng, F.G., 2007. Subgrain-size decoupling of Re and ^{187}Os within molybdenite. Mineral Deposits 26, 572–580 (in Chinese with English abstract).

Gao, B.Y., Xue, C.J., Chi, G.X., Li, C., Qu, W.J., Du, A.D., Li, Z.X., Gu, H., 2012. Re–Os dating of bitumen in the giant Jinding Zn–Pb deposit, Yunnan and its geological significance. Acta Petrologica Sinica 28, 1561–1567 (in Chinese with English abstract).

He, M.Q., Liu, J.J., Li, C.Y., Li, Z.M., Liu, Y.P., 2004. Mechanism of Ore-forming Fluids of the Lanping Pb–Zn–Cu Polymetallic Mineralized Concentration Area—An Example Study on the Baiyangping Ore District. Geological Publishing House, Beijing, pp. 1–108 (in Chinese with English abstract).

He, L.Q., Song, Y.C., Chen, K.X., Hou, Z.Q., Yu, F.M., Yang, Z.S., Wei, J.Q., Li, Z., Liu, Y.C., 2009. Thrust-controlled, sediment-hosted, Himalayan Zn–Pb–Cu–Ag deposits in the Lanping foreland fold belt, eastern margin of Tibetan Plateau. Ore Geology Reviews 36, 106–132.

Hou, Z.Q., Pan, G.T., Wang, A.J., Mo, X.X., Tian, S.H., Sun, X.M., Ding, L., Wang, E.Q., Gao, Y.F., Xie, Y.L., Zeng, P.S., Qin, K.Z., Xu, J.F., Qu, X.M., Yang, Z.M., Yang, Z.S., Fei, H.C., Meng, X.J., Li, Z.Q., 2006. Metallogenesis in Tibetan collisional orogenic belt: II. Mineralization in late-collisional transformation setting. Mineral Deposits 25, 521–543 (in Chinese with English abstract).

Hou, Z.Q., Khin, Z., Pan, G.T., Mo, X.X., Xu, Q., Hu, Y.Z., Li, X.Z., 2007. Sanjiang Tethyan metallogenesis in S.W. China: tectonic setting, metallogenic epochs and deposit types. Ore Geology Reviews 31, 48–87.

Hou, Z.Q., Song, Y.C., Li, Z., Wang, Z.L., Yang, Z.M., Yang, Z.S., Liu, Y.C., Tian, S.H., He, L.Q., Chen, K.X., Wang, F.C., Zhao, C.X., Xue, W.W., Lu, H.F., 2008. Thrust-controlled, sediments-hosted Pb–Zn–Ag–Cu deposits in the eastern and northern margins of Tibetan orogenic belt: geological features and tectonic model. Mineral Deposits 27, 123–144 (in Chinese with English abstract).

Jiang, S.Y., Slack, J.F., Palmer, M.R., 2000. Sm–Nd dating of the giant Sullivan Pb–Zn–Ag deposit, British Columbia. Geology 28, 751–754.

Ji, H.B., Li, C.Y., 1998. Geochemical characteristics and source of ore-forming fluid for the Jinman copper deposit in the western Yunnan Province, China. Acta Mineralogica Sinica 18, 28–37 (in Chinese with English abstract).

Khin, Z., Peters, S.G., Gromie, P., Burrett, C., Hou, Z.Q., 2007. Nature, diversity of the deposit types and metallogenic relations of South China. Ore Geology Reviews 31, 3–47.

Kosler, J., Simonetti, A., Sylvester, P.J., Cox, R.A., Tubrett, M.N., Wilton, D.H.C., 2003. Laser-ablation ICP-MS measurements of Re/Os in molybdenite and implications for Re–Os geochronology. Canadian Mineralogist 41, 307–320.

Kyle, J.K., Li, N., 2002. Jinding: a giant Tertiary sandstone-hosted Zn–Pb deposit, Yunnan, China. SEG Newsletter 50, 8–16.

Li, F., Fu, W.M., 2000. Geology of Red Bed Copper Deposits in Western Yunnan. Yunnan University Press, Kunming, p. 133 (in Chinese with English abstract).

Li, X.M., 2001. Metallogenic age of the Jinman copper deposit in the western Yunnan Province, China. Geoscience 15, 405–408 (in Chinese with English abstract).

Li, X.M., Song, Y.G., 2006. Cenozoic evolution of tectono-fluid and metallogenic process in the Lanping Basin, western Yunnan Province, Southwest China: constraints from apatite fission track data. Chinese Journal of Geochemistry 15, 405–408.

Liu, J.J., Li, C.Y., Zhang, Q., Pan, J.Y., Liu, Y.P., Liu, X.F., Liu, S.R., Yang, W.G., 2001. Wood textures in the Jinman Cu deposit in western Yunnan and their significance for ore genesis. Science in China (Series D) 31, 89–95 (in Chinese with English abstract).

Liu, J.J., Li, Z.M., Liu, Y.P., Li, C.Y., Zhang, Q., He, M.Q., Yang, W.G., Yang, A.P., Sang, H.Q., 2003. The metallogenic age of Jinman vein copper deposit, western Yunnan. Geoscience 17, 34–39 (in Chinese with English abstract).

Ludwig, R.K., 1996. ISOPLOT: A Plotting and Regression Program for Radiogenic-isotope Data (Version 2.9). U.S. Geological Survey Open-File Report 91-445, p. 47.

Luo, J.L., Yang, J.Z., 1994. The Tethyan Evolution and the Mineralization of the Main Metal Deposits in the Western Yunnan. Geological Publishing House, Beijing, pp. 149–239 (in Chinese with English abstract).

Mao, J.W., Xie, G.Q., Bierlein, F., Qu, W.J., Du, A.D., Ye, H.S., Pirajno, F., Li, H.M., Guo, B.J., Li, Y.F., Yang, Z.Q., 2008. Tectonic implications from the Re–Os dating of Mesozoic molybdenum deposits in the East Qinling–Dabie orogenic belt. Geochimica et Cosmochimica Acta 72, 4607–4626.

Misra, K.C., 2000. Understanding Mineral Deposits. Kluwer Academic Publishers, London, p. 845.

Mu, C.L., Wang, J., Yu, Q., Zhang, L.S., 1999. The evolution of the sedimentary basin in Lanping area during Mesozoic–Cenozoic. Mineral Petrology 19, 30–36 (in Chinese with English abstract).

Peng, J.T., Hu, R.Z., Burnard, P.G., 2003. Samarium-neodymium isotope systematics of hydrothermal calcites from the Xikuangshan antimony deposit (Hunan, China): the potential of calcite as a geochronometer. Chemical Geology 200, 129–136.

Qin, G.J., Zhu, S.Q., 1991. The ore-forming model of the Jinding lead–zinc deposit and prediction. Journal of Yunnan Geology 10, 145–190.

Selby, D., Creaser, A., 2004. Macroscale NTIMS and microscale LA-MC-ICP-MS Re–Os isotopic analysis of molybdenite: testing spatial restrictions for reliable Re–Os age determinations, and implications for the decoupling of Re and Os within molybdenite. Geochimica et Cosmochimica Acta 68, 3897–3908.

Shi, J.X., Yi, F.H., Wen, Q.D., 1983. The rock–ore characteristics and mineralization of the Jinding lead–zinc deposit, Lanping. Journal of Yunnan Geology 2, 179–195 (in Chinese with English abstract).

Shirey, S.B., Walker, R.J., 1995. Carius tube digestion for low blank rhenium–osmium analysis. Analytical Chemistry 67, 2136–2141.

Smoliar, M.I., Walker, R.J., Morgan, J.W., 1996. Re–Os ages of group IIA, IIIA, IVA and IVB iron meteorites. Science 271, 1099–1102.

Stein, H.J., Scherstén, K., Hannah, J.L., Markey, R., 2003. Subgrain-scale decoupling of Re and ^{187}Os and assessment of laser ablation ICP-MS spot dating in molybdenite. Geochimica et Cosmochimica Acta 92, 827–835.

Su, W.C., Hu, R.Z., Xia, B., Xia, Y., Liu, Y.P., 2009. Calcite Sm–Nd isochron age of the Shuiyindong Carlin-type gold deposit, Guizhou, China. Chemical Geology 258, 269–274.

Wang, Y.B., Chen, W., Zeng, P.S., 2005. Constraints of sericite ^{40}Ar–^{39}Ar ages on the metallogenic epoch of the Jinman vein copper deposit in the Lanping basin, northwestern Yunnan. Geological Bulletin of China 24, 181–184 (in Chinese with English abstract).

Wang, G.H., 2010. The Genetic Model of Liancheng–Jinman Vein-type Copper in the Lanping Basin, Yunnan Province. Master Report, Kunming University of Science and Technology, Kunming, p. 77 (in Chinese with English abstract).

Wang, X.H., Hou, Z.Q., Song, Y.C., Yang, T.N., Zhang, H.R., 2011. Baiyangping Pb–Zn–Cu–Ag polymetallic deposit in Lanping basin: metallogenic chronology and regional mineralization. Acta Petrologica Sinica 27, 2625–2634 (in Chinese with English abstract).

Xue, C.J., Chen, Y.C., Yang, J.M., Wang, D.H., 2002. Analysis of the ore-forming, background and tectonic system of the Lanping basin, Western Yunnan Province. Mineral Deposits 21, 36–44 (in Chinese with English abstract).

Xue, C.J., Chen, Y.C., Wang, D.H., Yang, J.M., Yang, W.G., 2003. Geology and isotopic composition of helium, neon, xenon and metallogenic age of the Jinding and Baiyangping ore deposits, northwest Yunnan. Science in China (Series D) 46, 789–800 (in Chinese with English abstract).

Xue, C.J., Zeng, R., Liu, S.W., Chi, G.X., Qing, H.R., Chen, Y.C., Yang, J.M., Wang, D.H., 2007. Geologic, fluid inclusion and isotopic characteristics of the Jinding Zn–Pb deposit, western Yunnan, South China: a review. Ore Geology Review 31, 337–359.

Xue, W., Xue, C.J., Chi, G.X., Gao, B.Y., Yang, S.F., 2010. Study on the fluid inclusions of Baiyangping poly-metallic deposit in Lanping Basin, northwestern Yunnan, China. Acta Petrologica Sinica 26, 1773–1784 (in Chinese with English abstract).

Xu, Q.D., Zhou, L., 2004. Ore-forming fluid migration in relation to mineralization zoning in Cu-polymetallic mineralization district of the northern Lanping, Yunnan: evidence from lead isotope and mineral chemistry of ores. Mineral Deposit 23, 452–463 (in Chinese with English abstract).

Xu, X.C., Huang, Z., Xie, Q.Q., Yue, S.C., Liu, Y., 2004. Ar–Ar isotopic ages of Jinman and Shuixie copper polymetallic deposits in Yunnan Province, and their geological implications. Geological Journal of China Universities 10, 157–164 (in Chinese with English abstract).

Zhang, C.J., Ni, S.J., Teng, Y.G., Peng, X.H., Liu, J.D., 2000. Relationship between Himalayan tectono-magmatic activity and mineralization in the Lanping basin. Mineral Petrol 20, 35–39 (in Chinese with English abstract).

Zhang, J.R., Wen, H.J., Qin, C.J., Wang, J.S., 2012. Fluid inclusion and stable isotopes study of Liancheng Cu–Mo polymetallic deposit in Lanping basin, Yunan Province. Acta Petrologica Sinica 28, 1373–1386 (in Chinese with English abstract).

Zhao, H.B., 2006. Study on the Characteristics and Metallogenic Conditions of Copper-polymetallic Deposits in Middle-northern Lanping Basin, Western Yunnan. Doctoral Report, China University of Geosciences, Beijing, p. 123 (in Chinese with English abstract).